


---

This is the **accepted version** of the journal article:

Herraiz-Martínez, Francisco Javier; Zamora González, Gerard; Paredes, Ferran; [et al.]. «Multiband printed monopole antennas loaded with Open Complementary Split Ring Resonators (OCSRRLs) for PANs and WLANs». IEEE antennas and wireless propagation letters, Vol. 10 (Dec. 2011), p. 1528-1531. DOI 10.1109/LAWP.2011.2181309

---

This version is available at <https://ddd.uab.cat/record/288469>

under the terms of the  **IN** COPYRIGHT license

# Multiband Printed Monopole Antennas loaded with Open Complementary Split Ring Resonators (OCSRRs) for PANs and WLANs

Francisco Javier Herraiz-Martínez, *Member, IEEE*, Gerard Zamora, Ferran Paredes, Ferran Martín, *Fellow, IEEE*, and Jordi Bonache, *Member, IEEE*

**Abstract**—Multiband printed monopole antennas loaded with open complementary split ring resonators (OCSRRs) are presented. The OCSRRs, modeled as parallel LC resonant tanks, act as high-impedance elements at their resonance frequencies, and different effective  $\lambda/4$  sections can be achieved in the monopole by placing them at proper locations. Thus, the first working frequency is related to the length of the monopole, while the additional bands are controlled by the resonance frequencies of the OCSRRs. Moreover, the proposed antennas present monopolar radiation characteristics at all the operation bands. Two prototypes are designed, manufactured and measured: (i) a single-loaded OCSRR dual-band printed monopole antenna covering the Bluetooth and IEEE 802.11a/b/g/n bands (2.40-2.48 GHz and 5.15-5.80 GHz, respectively), and (ii) a tri-band prototype based on the same design, but with an additional OCSRR designed to also cover the IEEE 802.11y frequency band (3.65-3.70 GHz). Both antennas are printed on a single-layer of a low-cost substrate, resulting very compact designs.

**Index Terms**— Metamaterials, monopole antenna, multifrequency antennas, printed antennas.

## I. INTRODUCTION

THE growing use of Wireless Local Area Networks (WLANs) and Personal Area Networks (PANs) requires the development of multiband antennas capable to operating to different standards and different frequency bands allocated for wireless communication systems. Moreover, the required antennas must be compact and low-cost in order to integrate them into terminals and access points. Printed monopole antennas satisfy all these requirements.

The conventional approach to achieve multiband printed monopoles consists of using several strips or creating different electric paths, each of them resonating at different frequencies [1]–[7]. Drawbacks of these designs are the increase of antenna dimensions, the need of large ground planes, or the difficulty to obtain the required operating frequencies due to antenna complexity. Recently, the use of LC resonator loading has been proposed to achieve multiband printed antennas. The simplest idea is based on loading a printed antenna with a set

of resonant particles [8]–[10]. This technique has been used to develop multiband printed dipole antennas [8],[9]. The resulting antennas exhibit two or more working bands. The first band is directly related to the printed antenna; the additional bands are determined by the loading elements. However, it was found that the bandwidth of these additional bands is very narrow due to the high Q factor of the magnetically coupled resonant particles considered. In [11], a dual-band printed monopole antenna with metamaterial-inspired reactive loading was designed. The loading induces an additional resonance in which the antenna acts as a radiating slot. Thus, the antenna does not present similar radiation characteristics at the two bands. A similar approach was proposed to design a tri-band printed monopole antenna [12], where the additional band was obtained by using a “defected” ground plane. However, the combination of different radiation mechanisms leads to orthogonal radiation patterns at the different bands, and the complexity and fabrication costs of this approach are higher due to the two printed layers and air bridges used in this design.

In this work, open complementary split ring resonators (OCSRRs) [13] are integrated inside a conventional monopole in order to implement novel multiband printed monopole antennas. The radiating element is always the monopole; hence, the radiation characteristics in terms of radiation pattern, polarization and gain are similar to those of a conventional printed monopole at all the operation bands. The resulting antennas are compact, single-layer and can be fabricated with low-cost techniques for mass production.

## II. ANTENNA DESIGN AND WORKING PRINCIPLE

### A. Dual-Band Printed Monopole Antenna

The proposed antenna is based on a rectangular printed monopole fed through a coplanar waveguide (CPW) transmission line (printed on the same substrate side), and loaded with an OCSRR at a distance  $d_o$  from the feeding point (Fig. 1a). The OCSRR (Fig. 1b) can be modeled as a series connected parallel LC resonator since there are two current paths between the two regions of the monopole separated by the OCSRR: (i) an inductive path through the central strip (of width  $d$ ) of the OCSRR, and (ii) a displacement current through the slots (of width  $c$ ) of the particle [13].

Manuscript received October 14, 2011. This work was supported by the Spanish MICINN (projects CSD2008-00066 and TEC2010-17512).

The authors are with GEMMA/CIMITEC, Departament d'Enginyeria Electrònica, Universitat Autònoma de Barcelona, Bellaterra (Barcelona), 08193, Spain (e-mail: fjherraiz@tsc.uc3m.es).

The working principle of the proposed antenna is similar to the one used in trap antennas [14]–[15]. The approach consists on inserting a LC parallel tank within the monopole. Out of resonance, the trap behaves as a reactive load which modifies the electrical length of the monopole. Thus, the first resonance occurs when the electrical length of the loaded antenna is  $\lambda/4$ . On the other hand, at the resonance frequency of the trap, the impedance at the trap is very high, and an open-circuit is seen at the trap position from the feeding point. Hence, if the trap is located at a convenient position (approximately  $\lambda/4$  from the feeding point at its resonance frequency), an additional radiating frequency is achieved. Hence, a dual-band monopole antenna is obtained.

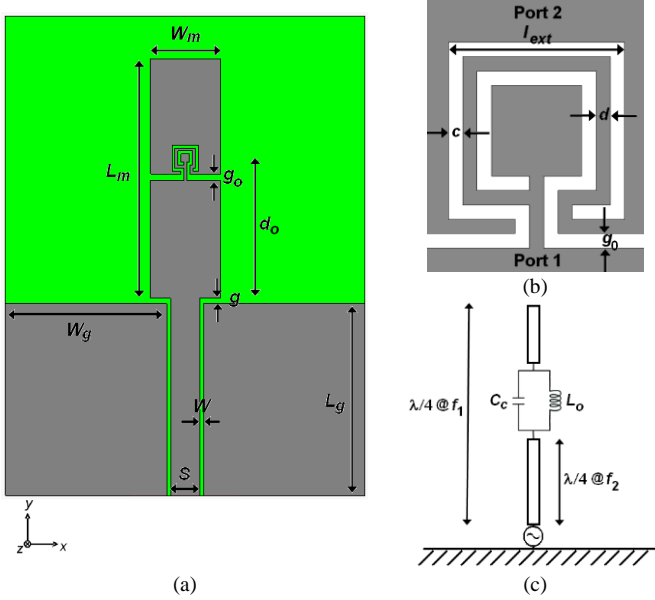


Fig. 1. Sketch of the proposed dual-band printed monopole antenna loaded with an OCSRR: (a) Top view of the proposed antenna, (b) zoom view of the OCSRR layout and (c) equivalent circuit model. Relevant dimensions are indicated.

Taking into account that the circuit model of the OCSRR is a LC parallel resonant tank [13], the proposed antenna can be described as shown in Fig. 1c. The inductance of the OCSRR,  $L_o$ , is the one of the metallic strip between the slots, and  $C_c$  takes into account the capacitive effects across the slots. Thus, the resonance frequency of the OCSRR,  $f_o$ , is given by:

$$f_o = \frac{1}{2\pi\sqrt{L_o C_c}} \quad (1)$$

The capacitance  $C_c$  is roughly the capacitance of a CSRR with identical dimensions and substrate, whereas the inductance  $L_o$  is four times larger [13]. The OCSRR is thus electrically smaller than the CSRR by a factor of two. According to these words, the resonance frequency of the OCSRR can be estimated from the CSRR model reported in [16].

In order to design a dual-band monopole antenna, the total electrical length of the monopole is set to  $\lambda/4$  at the first resonance frequency,  $f_1$ , whereas the OCSRR is placed at a distance of  $\lambda/4$  from the feeding point at  $f_2$ . The resonance frequency of the OCSRR corresponds to the second working frequency,  $f_2$ , hence  $f_o = f_2$  (the physical parameters of the OCSRR  $l_{ext}$ ,  $c$  and  $d$  are chosen in order to achieve such

resonance frequency). Indeed  $L_m$  must be slightly reduced since the OCSRR has an inductive behavior below its resonance frequency and thus, enlarges the electrical length of the monopole antenna.

Following this approach, a prototype of the proposed antenna has been designed to simultaneously cover the bands of 2.40–2.48 GHz (Bluetooth and WiFi) and 5.15–5.80 GHz (WiFi). The considered substrate is the low-cost FR4 ( $\epsilon_r = 4.5$  and  $h = 1.5$  mm). The final dimensions of the monopole are  $L_m = 21$  mm,  $W_m = 5.85$  mm. The parameters of the feeding line are set to obtain a 50- $\Omega$  CPW. Hence,  $S = 2.44$  mm and  $W = 0.30$  mm. The dimensions of each ground plane are  $L_g = 16$  mm and  $W_g = 13.48$  mm. The gap between the ground planes and the monopole is  $g = 0.30$  mm. The OCSRR is placed at a distance  $d_o = 12.50$  mm and its parameters are  $l_{ext} = 2.30$  mm,  $c = d = 0.25$  mm. The gap  $g_o$  is set to 0.50 mm.

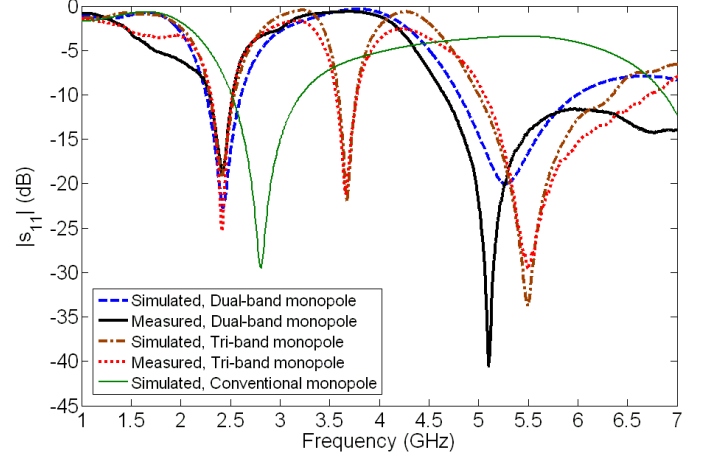


Fig. 2. Simulated and measured reflection coefficient of the proposed dual-band and tri-band printed monopole antennas. The simulated reflection coefficient of the conventional monopole antenna is also plotted.

Fig. 2 shows the simulated (CST ® Microwave Studio) reflection coefficient of the proposed dual-band monopole antenna. The reflection coefficient of the conventional monopole antenna (i.e., the same antenna without the OCSRR loading) is also shown for comparison. For the conventional monopole antenna, there is only one operating frequency band within the region of interest. This band is centered at 2.81 GHz. On the other hand, there are two resonances within the region of interest in the reflection coefficient of the OCSRR-loaded antenna. The first one is well matched from 2.26 GHz to 2.60, considering  $|S_{11}| < -10$  dB. This corresponds to a 14% fractional bandwidth, centered at 2.43 GHz. Following the same criteria, the second band goes from 4.81 GHz to 5.99 GHz. This second band is centered at 5.4 GHz. These results are consistent with the equivalent circuit model, because two resonances occur in the proposed antenna. Moreover, the first resonance is shifted down as compared to that of the unloaded monopole antenna due to the inductive behavior of the OCSRR below its resonance frequency; the second resonance appears at the resonance frequency of the OCSRR.

Fig. 3 shows the currents on the monopole antenna at the two resonances. At the first frequency (2.45 GHz), there are currents surrounding the OCSRR, but on the rest of the

monopole the current distribution is very similar to that of a conventional monopole antenna. All the currents are in-phase with maximum amplitude at the feeding point and minimum at the open edge of the antenna ( $\lambda/4$  current distribution). On the other hand, at the second resonance (5.40 GHz) all the currents on the upper part of the monopole are concentrated around the OCSRR and there are no currents beyond the particle position. Therefore, the particle acts as a trap. The currents on the lower part of the antenna exhibit a  $\lambda/4$  distribution, i.e., all the currents are in-phase with a maximum in the feeding point and a minimum at the separation gap between the two halves of the antenna. Thus, the effective radiation element is the monopole formed by the lower part of the antenna. Hence, a monopolar radiation pattern is expected at both frequency bands due to the effective monopolar current distributions.

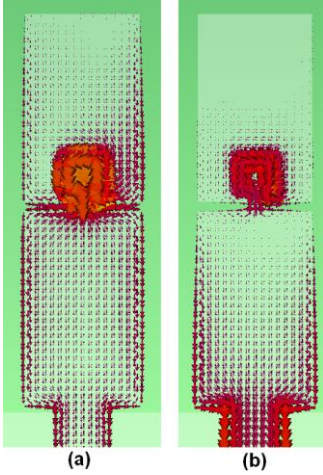


Fig. 3. Simulated electric currents on the proposed dual-band monopole antenna. (a) 2.45 GHz. (b) 5.40 GHz.

### B. Tri-Band Printed Monopole Antenna

The same approach can be used to design multi-frequency printed monopole antennas with more than two bands. The idea consists on introducing additional OCSRRs designed to exhibit the required frequencies and located at  $\lambda/4$  from the feeding point at the corresponding frequency (see the equivalent circuit for a tri-band monopole in Fig. 4a). In order to show the validity of the proposed approach, a tri-band monopole antenna has been designed. The tri-band monopole antenna is an extension of the previous dual-band antenna and it covers the previous bands and the IEEE 802.11y band of 3.65-3.70 GHz. According to the layout of the tri-band monopole (Fig. 4.b), the additional OCSRR is placed at a distance  $d_{o2} = 18.00$  mm. Its design parameters are  $l_{ext} = 2.70$  mm,  $c = d = 0.25$  mm. This corresponds to a resonance frequency of 3.65 GHz. The gap  $g_{o2}$  is set to 0.40 mm. These values have been optimized to only cover the desired bandwidth and not interfere with other systems. The other parameters of the antenna remain unchanged with respect to the dual-band design, except the length of the monopole which is reduced to  $L_m = 19.75$  mm to compensate the inductive behavior of the OCSRRs below their resonance frequencies. The simulated reflection coefficient of the tri-band monopole

antenna is also shown in Fig. 2. The antenna exhibits a behavior similar to the dual-band case, but it has an additional band, as expected. This band is centered at 3.66 GHz and it has a 6 % bandwidth. Hence, it covers the 802.11y band.

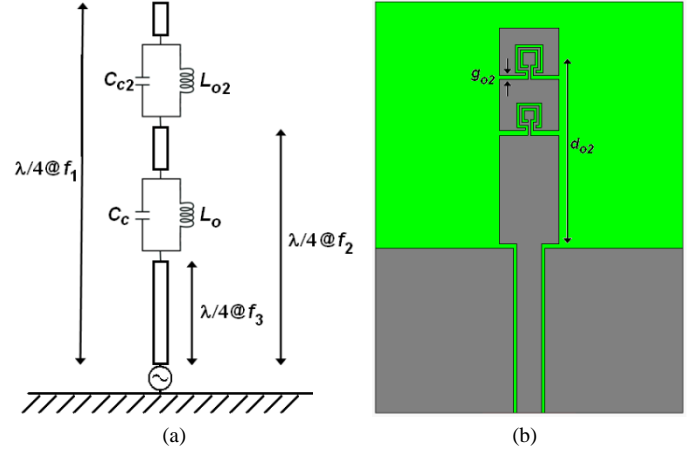


Fig. 4. (a) Equivalent circuit model of a tri-band printed monopole antenna loaded with two OCSRRs. (b) Sketch of the proposed tri-band printed monopole antenna loaded with OCSRRs.

## III. EXPERIMENTAL RESULTS

The proposed antennas have been fabricated and measured. Fig. 5 shows a picture of the two fabricated prototypes. The measured reflection coefficients are also plotted in Fig. 2. Good agreement between the simulated and experimental results is obtained. The fabricated dual-band printed monopole antenna exhibits good matching ( $|S_{11}| < -10$  dB) from 2.29 GHz to 2.52 GHz at the lower frequency band. This corresponds to a 9.6% bandwidth. In the upper band, the antenna is well matched from 4.66 GHz to at least 7 GHz. Thus, the fabricated antenna satisfies the specifications of Bluetooth and WiFi (bands of 2.40-2.48 GHz and 5.15-5.80 GHz).

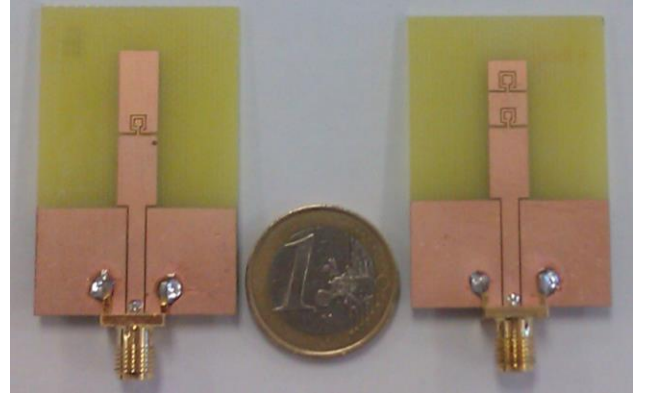


Fig. 5. Picture of the fabricated prototypes.

The fabricated tri-band monopole antenna is well matched from 2.30 GHz to 2.52 GHz for the first band. Its reflection coefficient is below -10 dB between 3.56 GHz and 3.78 GHz for the second band, and between 5.06 GHz and 6.71 GHz for the third band. Hence, the fabricated prototype is well matched within the regulated bandwidths of Bluetooth and WiFi including IEEE 802.11y (3.65-3.70 GHz band).

The proposed antennas present monopolar radiation

characteristics at all the bands. As an example, the normalized measured radiation patterns of the tri-band monopole antenna are shown in Fig. 6. A monopolar radiation pattern is obtained at the three frequencies. The crosspolar component (XPOL) has low values (below -20 dB in all of the cases, except the XY plane of the third frequency where is below -15 dB). The gains of this design are 1.4 dB, 1.2 dB and 1.7 dB at the first, second and third bands, respectively.

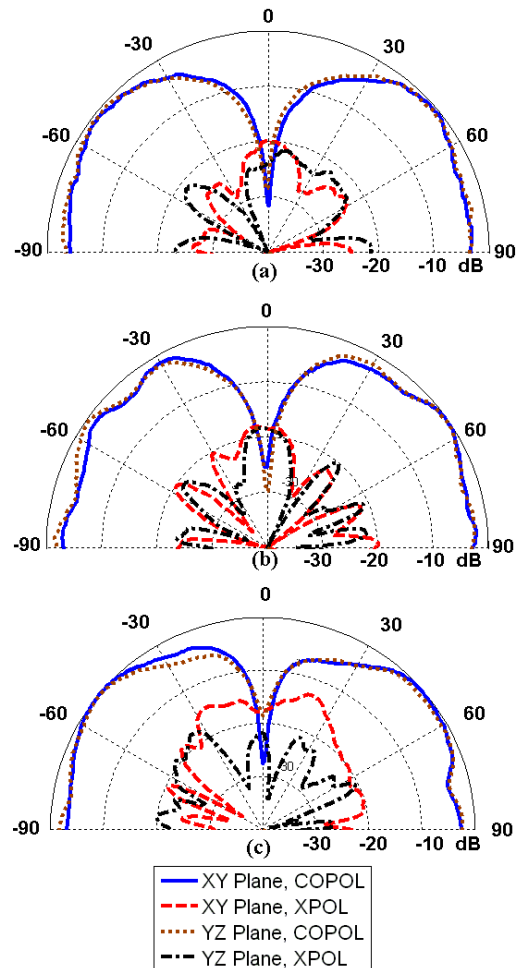


Fig. 6. Measured radiation patterns of the tri-band printed monopole antenna. (a) 2.45 GHz, (b) 3.65 GHz, (c) 5.40 GHz.

#### IV. CONCLUSION

Multiband printed monopole antennas loaded with OCSRRs have been proposed. The operation principle of these antennas is similar to the one of trap monopole antennas, which has been extensively used at HF frequencies for many years. Two or more operating bands at non-harmonic frequencies can be obtained through the proposed approach, and the working frequencies are closely related to the length of the monopole and to the resonance frequency of the loading OCSRRs. In order to show the validity of the proposed approach, two prototypes have been fabricated and characterized: the first one, a dual-band antenna based on a printed monopole loaded with a single OCSRR has been found to be suitable for Bluetooth and WiFi (bands of 2.40-2.48 GHz and 5.15-5.80 GHz). The second prototype is an extension of the previous one and includes an additional OCSRR in order to also cover

the IEEE 802.11y frequency band. The proposed antennas exhibit radiation characteristics similar to those of conventional monopole antennas at all the operating bands. These antennas have been implemented on a single layer of a low-cost substrate without non-planar elements. The overall dimensions of the board are always below 30 mm x 40 mm x 1.5 mm. These OCSRR-based antennas can be of interest for modern PANs and WLANs.

#### REFERENCES

- [1] Y.-L. Kuo, and K.-L. Wong, "Printed double-T monopole antenna for 2.4/5.2 GHz dual-band WLAN operations," *IEEE Transactions on Antennas and Propagation*, vol. 51, no. 9, pp. 2187-2192, September 2003.
- [2] W.-C. Liu, W.-R. Chen, and C.-M. Wu, "Printed double S-shaped monopole antenna for wideband and multiband operation of wireless communications," *IEE Proceedings-Microwaves, Antennas and Propagation*, vol. 151, no. 6, pp. 473-476, December 2004.
- [3] M. J. Ammann, and R. Farrell, "Dual-band monopole antenna with stagger-tuned arms for broadbanding," *IEEE International Workshop on Antenna Technology: Small Antennas and Novel Metamaterials (IWAT 2005)*, pp. 278-281, 2005.
- [4] M. John, and M. J. Ammann, "Integrated antenna for multiband multinational wireless combined with GSM1800/PCS1900/IMT2000 + extension," *Microwave and Optical Technology Letters*, vol. 48, no. 3, pp. 613-615, March 2006.
- [5] Y. Ge, K. P. Esselle, and T. S. Bird, "Compact triple-band multi-band monopole antenna," *2006 IEEE International Workshop on Antenna Technology: Small Antennas and Novel Metamaterials (IWAT 2006)*, pp. 172-175, 2006.
- [6] H. Wang, "Dual-resonance monopole antenna with tuning stubs," *IEE Proceedings-Microwaves, Antennas and Propagation*, vol. 153, no. 4, pp. 395-399, August 2006.
- [7] H. Wang, and M. Zheng, "Triple-band wireless local area network monopole antenna," *IET Microwaves, Antennas and Propagation*, vol. 2, no. 4, pp. 367-372, 2008.
- [8] F. J. Herraiz-Martínez, L. E. García-Muñoz, D. González-Ovejero, V. González-Posadas and D. Segovia-Vargas, "Dual-frequency printed dipole loaded with Split Ring Resonators", *IEEE Antennas and Wireless Propagation Letters*, vol. 8, pp. 137-140, 2009.
- [9] D. Segovia-Vargas, F. J. Herraiz-Martínez, E. Ugarte-Muñoz, J. Montero-de-Paz, V. González-Posadas and L. E. García-Muñoz, "Multifrequency Printed Antennas Loaded with Metamaterial Particles", *Radioengineering*, vol. 18, no. 2, pp. 129 - 143, June 2009.
- [10] J. Montero-de-Paz, E. Ugarte-Muñoz, F. J. Herraiz-Martínez, V. González-Posadas, L. E. García-Muñoz and D. Segovia-Vargas, "Multifrequency self-diplexed single patch antennas loaded with Split Ring Resonators", *Progress in Electromagnetics Research*, vol. 113, pp. 47-66, 2011.
- [11] J. Zhu, and G. V. Eleftheriades, "Dual-band metamaterial-inspired small monopole antenna for WiFi applications," *Electronics Letters*, vol. 45, no 22, pp. 1104-1106, October 2009.
- [12] J. Zhu, M. A. Antoniades, and G. V. Eleftheriades, "A compact tri-band monopole antenna with single-cell metamaterial loading," *IEEE Transactions on Antennas and Propagation*, vol. 58, no. 4, pp. 1031-1038, April 2010.
- [13] A. Vélez, F. Aznar, J. Bonache, M. C. Velázquez-Ahumada, J. Martel, and F. Martín, "Open Complementary Split Ring Resonators (OCSRRs) and their application to wideband CPW band pass filters," *IEEE Microwave and Wireless Components Letters*, vol. 19, no. 4, pp. 197-199, April 2009.
- [14] The ARRL Antenna Book, R. D. Straw, E., 21<sup>st</sup> ed. Newington, CT: Nat. Assoc. Amateur Radio, 2007.
- [15] D. L. Smith, "The trap-loaded cylindrical antenna," *IEEE Transactions on Antennas and Propagation*, vol. 23, no. 1, pp. 20-27, January 1975.
- [16] J.D. Baena, J. Bonache, F. Martín, R. Marqués, F. Falcone, T. Lopetegui, M.A.G. Laso, J. García, I. Gil, M. Flores-Portillo and M. Sorolla, "Equivalent circuit models for split ring resonators and complementary split rings resonators coupled to planar transmission lines", *IEEE Transactions on Microwave Theory and Techniques*, vol. 53, pp. 1451-1461, April 2005.